



## SYNTHESIS OF GROUND MOTIONS OF A LOMA PRIETA-TYPE EARTHQUAKE IN THE VICINITY OF THE SAN FRANCISCO METROPOLITAN AREA

G. DEODATIS<sup>1</sup>, E. DURUKAL<sup>2</sup>, A.S. PAPAGEORGIU<sup>3</sup>, M. SHINOZUKA<sup>4</sup>

<sup>1</sup> Dept. of Civil Engineering and Operations Research, Princeton University, Princeton, NJ 08544, USA

<sup>2</sup> Dept. of Earthquake Engineering, Bogazici University, 81220 Cengelkoy, Istanbul, Turkey

<sup>3</sup> Dept. of Civil Engineering, Rensselaer Polytechnic Institute, Troy, NY 12180, USA

<sup>4</sup> Dept. of Civil Engineering, University of Southern California, Los Angeles, CA 90089, USA

### ABSTRACT

In this paper, seismic ground motion in the form of displacement time histories is synthesized using a discrete wave number approach in conjunction with a propagator-based formalism. The synthesized earthquake event considers the rupture of a 40 km long segment of the San Andreas fault, close to San Francisco. The choice of this particular segment of the San Andreas fault is made because of its high probability for a magnitude 7 earthquake in the next 30 years, and its proximity to the San Francisco metropolitan area. Traces of particle motions on the horizontal plane are computed at several points on the ground surface.

### KEYWORDS

Discrete wave number approach, synthesis of ground motion, San Andreas fault, Loma Prieta earthquake.

### INTRODUCTION

The  $M=7.1$  Loma Prieta earthquake of October 17, 1989 struck the San Francisco Bay area causing 62 deaths, 3,757 injuries and over \$6 billion in property damage. This area has been affected by five  $M \geq 7$  earthquakes since 1812. The 1838 ( $M \sim 7$ ) and 1906 ( $M \sim 8$ ) earthquakes were associated with the portion of the San Andreas fault in the San Francisco peninsula. The event of 1865 was probably associated with the same segment of the San Andreas fault as the Loma Prieta earthquake. The probability of one or more magnitude 7 or larger earthquakes along any of the faults in the San Francisco Bay region (specifically, the San Andreas, Hayward, and Rodgers Creek faults) in the coming 30 years is estimated to be about 0.67 by the Working Group on California Earthquake Probabilities (1990). In this paper, seismic ground motion will be synthesized due to the rupture of the 40 km long segment of the San Andreas fault indicated in Fig. 1. The 30 year probability for a magnitude 7 earthquake on this segment is estimated to be 0.23. The choice of this particular segment of the San Andreas fault was made because of this high probability and because of the high economic and social importance of the region.

### METHODOLOGY

A discrete wave number approach in conjunction with a propagator-based formalism will be used for the synthesis of seismic ground motion (Deodatis, Shinozuka and Papageorgiou 1990, Theoharis and Deodatis 1994, and Zhang and Deodatis 1996). This methodology is based on the work of Lamb (1904), Bouchon (1979),

Chouet (1987), and Dunkin (1965). The discrete wave number technique is used to propagate waves due to the rupture of an extended seismic source through a 3-D layered half-space. The method is deterministic in the description of the wave propagation. It can be probabilistic or deterministic in the description of the rupture of the seismic source. With this method, it is possible to calculate the near-field and the far-field seismic ground motion at any point of a layered viscoelastic half-space, such that the spatial variability of ground motion at distances comparable to the dimensions of engineering structures can be estimated. All types of waves (body and surface) are accounted for in the formulation of the problem. Ground motion time histories with frequency content up to 3 Hz can be calculated. The extent and magnitude of permanent ground deformation can also be computed, which is very important in the earthquake response of large scale engineering structures with relatively low natural frequencies of vibration, such as bridges.

In very broad terms, the problem consists of solving the equation:

$$u(x, y, t) = \int_{-\infty}^{\infty} \int_{-\infty}^{\infty} \int_{-\infty}^{\infty} \tilde{u}(\kappa_x, \kappa_y, \omega) \exp[-i\kappa_x x - i\kappa_y y + i\omega t] d\kappa_x d\kappa_y d\omega \quad (1)$$

where  $u(x, y, t)$  is the displacement field in the space-time domain, and  $\tilde{u}(\kappa_x, \kappa_y, \omega)$  are the complex Fourier amplitudes of the displacement field in the wave number-frequency domain. Closed-form analytic expressions are established for  $\tilde{u}(\kappa_x, \kappa_y, \omega)$ , and a (computationally expensive) inverse triple Fourier transform must be performed to go from the wave number-frequency domain  $(\kappa_x, \kappa_y, \omega)$  to the space-time domain  $(x, y, t)$ .

The wave radiation from the source is decoupled into P-SV and SH motions and the two problems are then treated separately (3-D plane wave propagation) using the propagator-based formalism of Chouet (1987). Analytical expressions established for the displacements due to unidirectional unit impulses are used to compute the solutions for double couples associated with a strike-slip and a dip-slip fault. These solutions are finally combined and integrated over the fault area to yield  $\tilde{u}(\kappa_x, \kappa_y, \omega)$  in Eq. (1).

The problem requires a detailed description of both the ground and the seismic source. As far as the ground is concerned, information is needed for the thickness, S-wave velocity, P-wave velocity, density, and attenuation factor  $Q$  of each layer characterizing the earth structure in the study area.

The seismic source is described in terms of its dimensions and location within the earth structure, and in terms of its rupture pattern. The source can be either in one of the layers, or in the half-space. The source is discretized into a number of point sources, each one modeled by a double couple. Each double couple can have a different final slip (strike slip, dip slip, or a combination of the two), a different rise time, and a different rupture initiation time.

The evolution of the slip at a certain location on the fault plane as a function of time is described by the dislocation function. Haskell's model uses a ramp function for the dislocation whose Fourier transform in the frequency domain is given by:

$$F(\omega) = \frac{1}{\omega^2 t_r} [\exp(-i\omega t_r) - 1] + \pi \delta(\omega) \exp(-i\omega \frac{t_r}{2}) \quad (2)$$

where  $\omega$  is the frequency in rad/s,  $t_r$  is the rise time in seconds, and  $\delta(\omega)$  is Dirac's delta function.

Papageorgiou and Aki (1983) define the dislocation function at a distance  $r$  from the center of the circular sub-fault at time instant  $t$  as:

$$\Delta u(r, t, t_i) = C \sigma_e \frac{v_s}{\mu} \sqrt{(t - t_i)^2 - \frac{r^2}{v^2}} H \left( t - t_i - \frac{r}{v} \right) \quad \text{for } t < t_r \quad (3a)$$

$$\Delta u(r, t, t_i) = C \sigma_e \frac{v_s}{\mu} \sqrt{(t_r - t_i)^2 - \frac{r^2}{v^2}} \quad \text{for } t > t_r \quad (3b)$$

with:

$$t_r = t_i + \frac{r_0}{v} + \frac{r_0 - r}{v_h} \quad (3c)$$

where  $C$  is a parameter depending on the shear wave velocity and the rupture velocity,  $\sigma_e$  is the effective stress,  $v$  is the rupture velocity,  $v_s$  is the shear wave velocity,  $v_h$  is the healing velocity,  $\mu$  is the rigidity of the medium,  $r_0$  is the radius of each circular sub-fault,  $t_i$  is the time rupture starts at the center of the sub-fault,  $t_r$  is the rise time and  $H$  is the Heavyside unit step function. There is no closed-form analytical expression for the

Fourier transform of the expression shown in Eq. (3) due to its complexity. It can be approximated, however, by a series of  $n_s$  line segments, leading to the expression:

$$F(\omega) = \frac{C\sigma_e v_s}{\Delta u_F \mu v} \left[ \frac{1}{i\omega} \exp\left(-i\omega \frac{r'_0}{v}\right) \sqrt{r_0'^2 - r^2} + \sum_{k=1}^{n_s} \left\{ \frac{1}{i\omega} \left[ \exp\left(-i\omega \frac{\rho_{k-1}}{v}\right) - \exp\left(-i\omega \frac{\rho_k}{v}\right) \right] \sqrt{\rho_{k-1}^2 - r^2} + \left( \sqrt{\rho_k^2 - r^2} - \sqrt{\rho_{k-1}^2 - r^2} \right) \left[ \frac{v}{\omega^2(\rho_k - \rho_{k-1})} \exp\left(-i\omega \frac{\rho_{k-1}}{v}\right) \cdot \left[ \exp\left(-i\omega \frac{(\rho_k - \rho_{k-1})}{v}\right) - 1 \right] - \frac{1}{i\omega} \exp\left(-i\omega \frac{\rho_k}{v}\right) \right] \right\} \right] + \pi\delta(\omega) \quad (4a)$$

where:

$$\rho_k = r + k \frac{r'_0 - r}{n_s} \quad ; \quad r'_0 = r_0 + \frac{r_0 - r}{v_h} v \quad ; \quad k = 0, 1, \dots, n_s \quad (4b)$$

and  $\Delta u_F$  being the final slip at a distance  $r$  from the center of the circular sub-fault. For  $n_s = 1$ , the expression in Eq. (4a) can be simplified with great accuracy as:

$$F(\omega) = \frac{C\sigma_e v_s}{\Delta u_F \omega^2 \mu} \sqrt{\frac{r'_0 + r}{r'_0 - r}} \exp\left(\frac{-i\omega r}{v}\right) \left[ \exp\left(\frac{-i\omega(r'_0 - r)}{v}\right) - 1 \right] + \pi\delta(\omega) \quad (5a)$$

with:

$$r'_0 = t_r v \quad (5b)$$

$$r = r_0 - \left(t_r - \frac{r_0}{v}\right) v_h \quad (5c)$$

Denoting now by  $\Delta u$  the following ratio:

$$\Delta u = \frac{\Delta u_F}{\Delta u_F^{\text{center}}} \quad (6)$$

where  $\Delta u_F^{\text{center}}$  is the final slip at the center of the sub-fault, it can be shown that  $\Delta u$  and  $t_r$  are related as:

$$t_r = \frac{\frac{-2r_0 v_h}{v^2} \left(1 + \frac{v_h}{v}\right) + \sqrt{4r_0^2 \left(1 + \frac{v_h}{v}\right) \left[ \left(1 + \frac{v_h}{v}\right) \frac{1}{v^2} + \Delta u^2 \left(1 - \frac{v_h}{v}\right) \left(\frac{1}{v} + \frac{1}{v_h}\right)^2 \right]}}{2 \left(1 - \frac{v_h^2}{v^2}\right)} \quad (7)$$

## SYNTHESIS OF GROUND MOTION

For the scenario earthquake considered in this study, it is assumed that a 40 km long by 10 km deep portion of the San Andreas fault would rupture during such an event. The rupturing segment relative to the San Francisco Bay area is shown in Fig. 1.

An earth model including the Moho discontinuity is considered. The layering of the ground is shown in Fig. 2 with all the numerical values of the parameters describing the problem.

A barrier model with irregular boundaries has been utilized to calculate the distribution and the amount of the final slip over the fault plane. The details of this barrier model with irregular boundaries will be provided in an upcoming paper. The basic idea is that an underlying barrier model with regular circular boundaries is transformed into a corresponding one with irregular boundaries using the spectral representation method for simulation of stochastic fields. For the purposes of this case study, it is assumed that the underlying barrier model with regular circular boundaries consists of four circular sub-faults of 5,000 m radius each. The corresponding model with irregular boundaries is shown in Fig. 3. The rupture velocity is taken to be 2,000 m/s. The healing velocity is 2,200 m/s. Two types of dislocation functions are considered: the classic Haskell type ramp function and the dislocation function of Papageorgiou and Aki (1983) for the specific barrier model. The corresponding rise times for the barrier model with irregular boundaries shown in Fig. 3 are calculated using the formula in Eq. (7).

The source is discretized into  $65 \times 17$  point sources, each with a different amount of final slip and with a different rise time. As indicated in Fig. 3, the maximum final slip is 10.50 m, and the minimum (non-zero) final slip is 2.79 m. The maximum rise time is 4.8 s, and the minimum rise time is 2.6 s. The fault plane is vertical ( $\delta = 90^\circ$ ).

Three different cases of circular rupture patterns are considered. These three cases, displayed graphically in Table 1, differ in the location of the hypocenter.

Two cases are considered regarding the relative final amounts of strike slip versus dip slip. A case with strike slip only, where the final values for the slip are obtained using the barrier model with irregular boundaries for an  $M=7.0$  earthquake (see Fig. 3). And a case with equal amount of strike and dip slip, where the same final slip values as in the previous case are assumed for both the strike and dip directions.

As far as the computational parameters associated with the triple Fourier transform shown in Eq. (1) are concerned,  $512 \times 512$  wave numbers are used in the wave number domain with an upper cut-off wave number of 0.000947 rad/m, and 128 frequencies are used in the frequency domain with an upper cut-off frequency of 0.5 Hz.

Displacement traces and particle motions are computed at the seven locations indicated in Fig. 1. The first five points correspond to the abutments of two bridges in the area, point 6 is in San Francisco, and point 7 is in Oakland. Figure 4 displays displacement time histories in the directions parallel to the fault trace and perpendicular to the fault trace, at points 1 and 3 for the 7 cases described in Table 1. Figure 5 displays the traces of particle motions on the horizontal plane at points 3, 4 and 5.

At this juncture, it should be mentioned that the results shown in Figs. 4 and 5 are the first ones from a series of case studies that will be considered as part of a sensitivity analysis to examine the effects of several parameters involved in the problem.




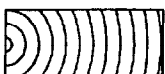

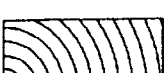
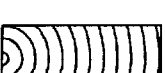
#### ACKNOWLEDGMENTS

All numerical computations in this study were carried out on the CRAY T3D machine at the Pittsburgh Supercomputing Center under Grant BCS930004P. This work was also supported by the National Science Foundation under Grant # BCS-9257900 with Dr. Clifford J. Astill as Program Director, and by the NCEER Highway Project (FHWA Contract DTFH61-92-C-00106).

#### REFERENCES

- Bouchon, M. (1979). "Discrete Wave Number Representation of Elastic Wave Fields in Three-Dimensional Space," *Journal of Geophysical Research*, Vol. 84, No. B7, pp. 3609-3614.
- Chouet, B. (1987). "Representation of an Extended Seismic Source in a Propagator Based Formalism," *Bulletin of the Seismological Society of America*, Vol. 77, No. 1, pp. 14-27.
- Deodatis, G., Shinozuka, M. and Papageorgiou, A.S. (1990). "Stochastic Wave Representation of Seismic Ground Motion. I: F-K Spectra," *Journal of Engineering Mechanics*, ASCE, Vol. 116, No. 11, pp. 2363-2379.
- Dunkin, J.W. (1965). "Computation of modal solutions in layered, elastic media at high frequencies," *Bulletin of the Seismological Society of America*, Vol. 55, No. 2, pp. 335-358.
- Lamb, H. (1904). "On the Propagation Tremors at the Surface of an Elastic Solid," *Philosophical Transactions of the Royal Society of London*, Vol. A203, pp. 1-42.
- Papageorgiou, A.S. and Aki, K. (1983). "A Specific Barrier Model for the Quantitative Description of Inhomogeneous Faulting and the Prediction of Strong Ground Motion. I: Description of the Model," *Bulletin of the Seismological Society of America*, Vol. 73, No. 3, pp. 693-722.
- Theoharis, A. and Deodatis, G. (1994). "Seismic Ground Motion in a Layered Half-space due to a Haskell-type source. I: Theory," *Soil Dynamics and Earthquake Engineering*, Vol. 13, No. 4, pp. 281-292.
- Working Group on California Earthquake Probabilities. (1990). "Probabilities of Large Earthquakes in the San Francisco Bay Region, California," US Geological Survey Circular 1053.
- Zhang, R. and Deodatis, G. (1996). "Seismic Ground Motion Synthetics of the 1989 Loma Prieta Earthquake," *accepted for publication in Earthquake Engineering and Structural Dynamics*.

Table 1. Description of cases considered.

	<i>Slip Type</i>	<i>Rupture Pattern</i>	<i>Dislocation Function</i>
Case 1	Strike slip		Ramp function
Case 2	Strike slip		Barrier model (as described in text)
Case 3	Strike slip		Barrier model (as described in text)
Case 4	Strike slip		Barrier model (as described in text)
Case 5	Strike slip-Dip slip		Barrier model (as described in text)
Case 6	Strike slip-Dip slip		Barrier model (as described in text)
Case 7	Strike slip-Dip slip		Barrier model (as described in text)

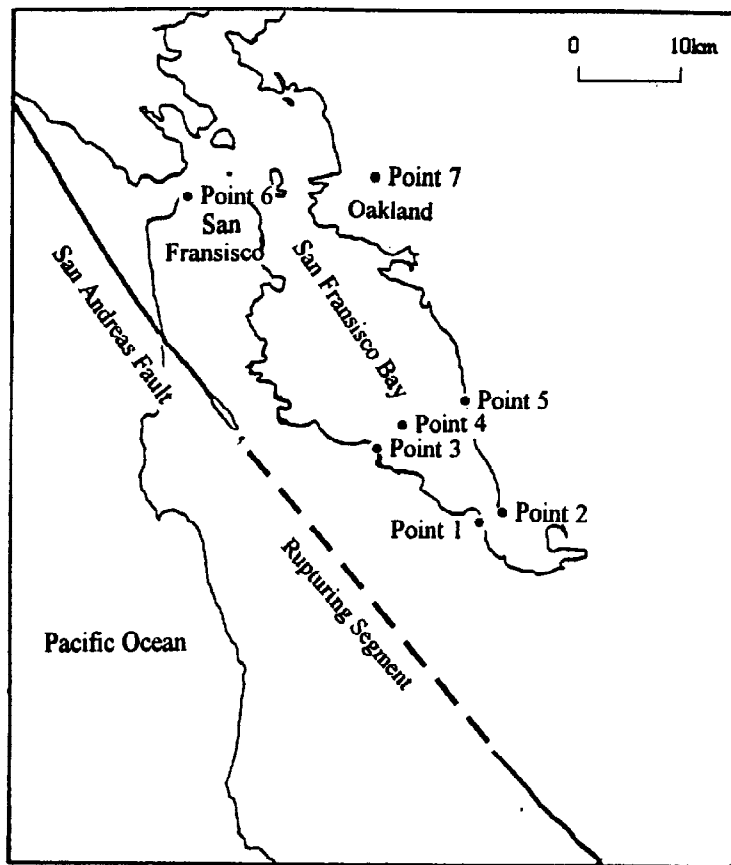


Fig. 1 The 40 km long rupturing segment of the San Andreas fault and the location of the seven points considered in this study.

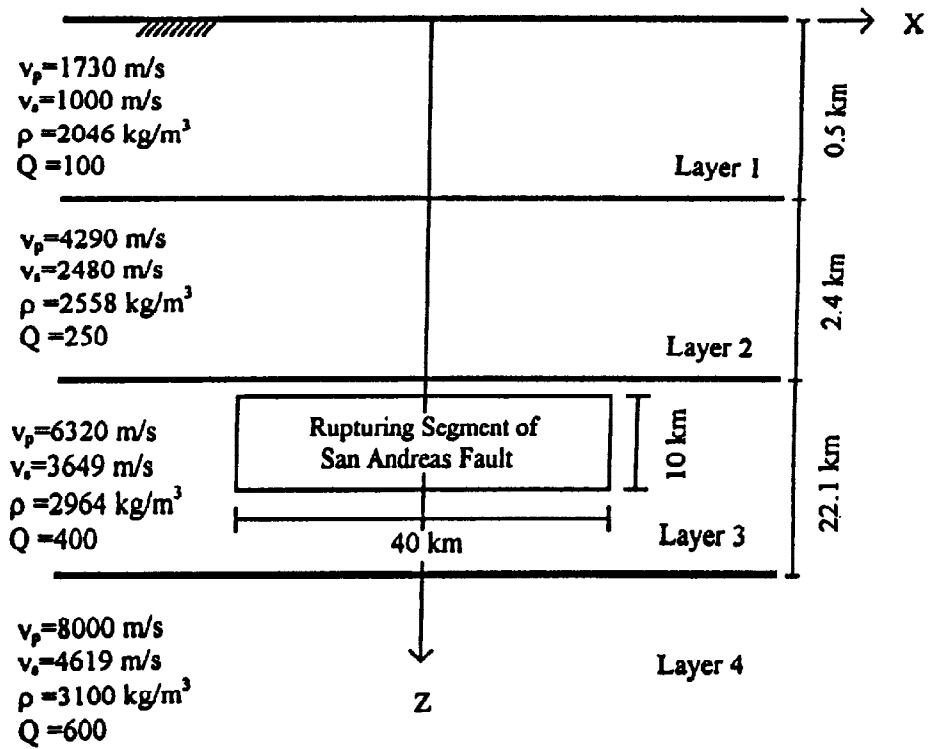


Fig. 2 Layering of the ground.

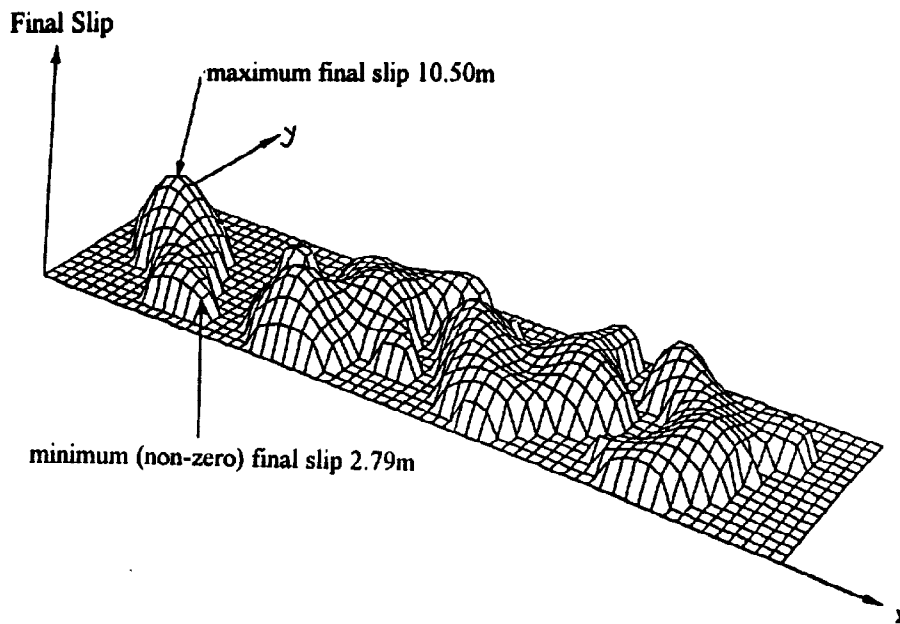


Fig. 3 Distribution and amount of final slip over the fault plane using a barrier model with irregular boundaries ( $M=7$ ).

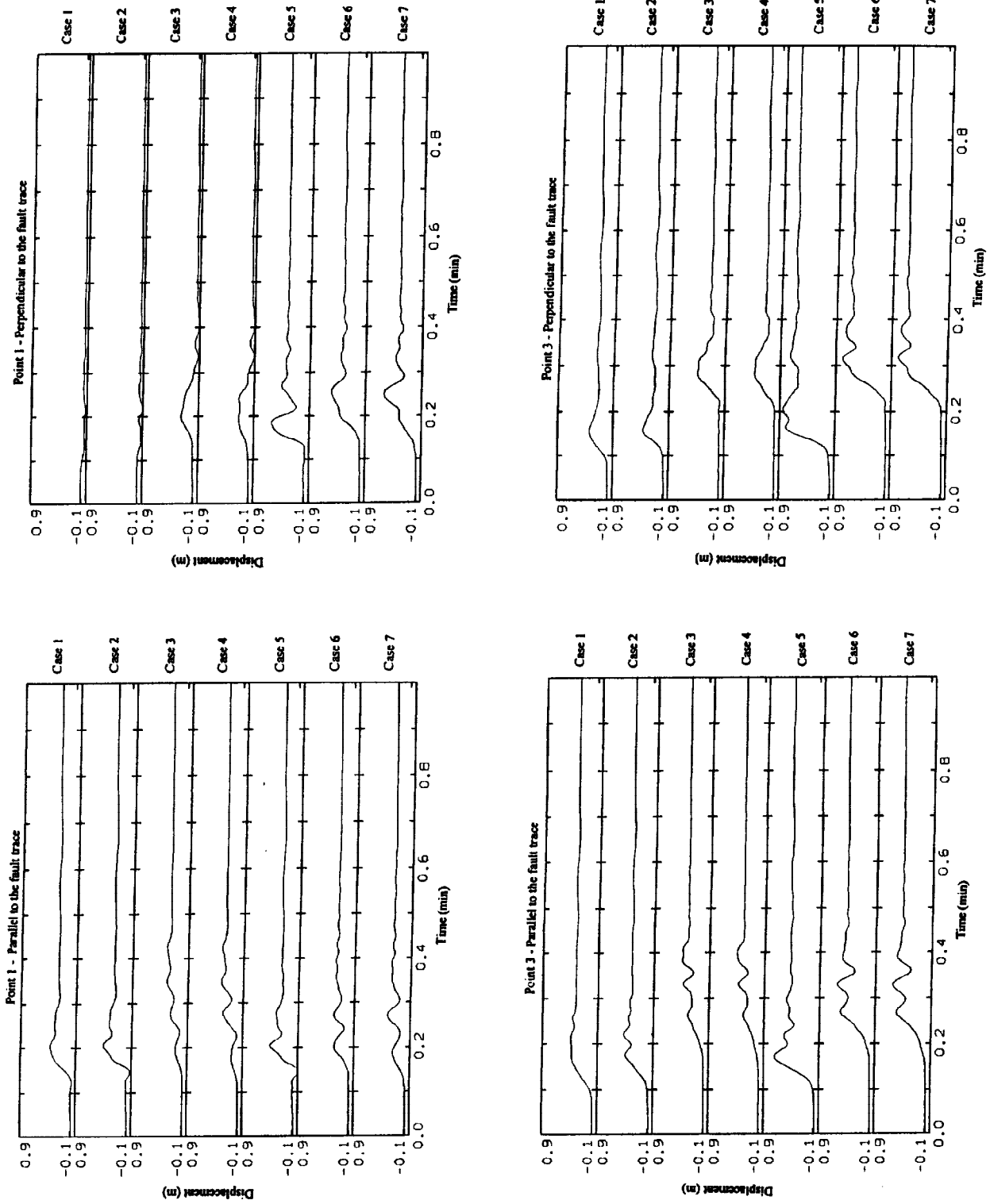


Fig. 4 Displacement time histories at points 1 and 3, for the seven cases considered in this study.

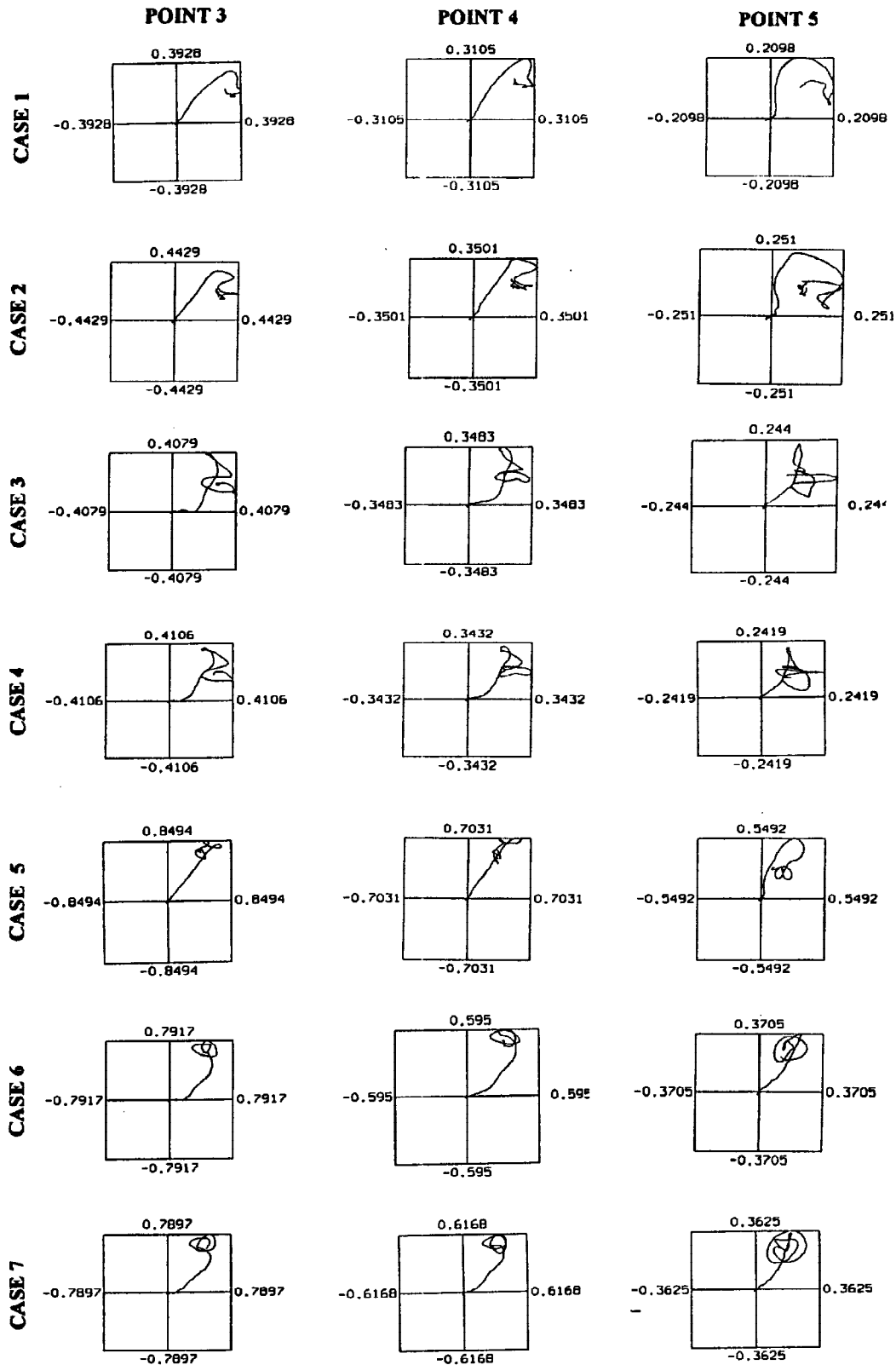


Fig. 5 Traces of particle motions on the horizontal plane at points 3, 4 and 5, for the seven cases considered in this study. The horizontal axis represents the direction parallel to the fault trace. The vertical axis is perpendicular to the fault trace. All numerical values are in meters.